Single-cell heterogeneity in ribosome content and the consequences for the growth laws

Leandra Brettner[1]*, Kerry Geiler-Samerotte[1,2]*

[1]Biodesign Institute Center for Mechanisms of Evolution, Arizona State University, Tempe, Arizona, USA
[2]School of Life Sciences, Arizona State University, Tempe, Arizona, USA
*correspondence: kerry.samerotte@asu.edu, leandra.brettner@asu.edu

ABSTRACT

Previous work has suggested that the ribosome content of a cell is optimized to maximize growth given the nutrient availability. The resulting correlation between ribosome number and growth rate appears to be independent of the rate limiting nutrient and has been reported in many organisms. The robustness and universality of this observation has given it the classification of a "growth law." These laws have had powerful impacts on many biological disciplines. They have fueled predictions about how organisms evolve to maximize reproduction, and informed models about how cells regulate growth. Due to methodological limitations, this growth law has rarely been studied at the level of individual cells. While *populations* of fast-growing cells tend to have more ribosomes than *populations* of slow-growing cells, it is unclear if individual cells tightly regulate their ribosome content to match their environment. Here, we use recent ground-breaking single-cell RNA sequencing techniques to study this growth law at the single-cell level in two different microbes, *S. cerevisiae* (a single-celled yeast and eukaryote) and *B. subtilis* (a bacterium and prokaryote). In both species, we find enormous variation in the ribosomal content of single cells that is not predictive of growth rate. Fast-growing populations include cells showing transcriptional signatures of slow growth and stress, as do cells with the highest ribosome content we survey. Broadening our focus to the levels of non-ribosomal transcripts reveals subpopulations of cells in unique transcriptional states suggestive of divergent growth strategies. These results suggest that single-cell ribosome levels are not finely tuned to match population growth rates or nutrient availability, at least not in a way that can be captured by a unifying law that applies to all cell types. Overall, this work encourages the expansion of these "laws" and other models that predict how growth rates are regulated or how they evolve to consider single-cell heterogeneity.

INTRODUCTION

Growth laws describe robust correlations between cell growth and other phenotypes[1–4]. Perhaps one of the most well-studied growth laws pertains to the relationship between cell growth and the ribosome[5,6]. Numerous studies have shown that faster growing populations of cells possess more ribosomes[7–9]. This makes intuitive sense as ribosomes make most of the components that cells need to grow and replicate. However, ribosomes are expensive, being composed of many proteins and rRNA molecules, and comprising a large portion of the transcriptome[10–14]. Thus, cell populations are thought to tightly optimize ribosome levels to match their environment[15,16]. This tight optimization has been demonstrated at the transcriptional level; ribosomal as well as many other growth-supporting transcripts respond in concert to changes in nutrient abundance or environment quality[17,18], sometimes within minutes[7]. The optimization of ribosome levels to match cell growth rate has been observed across diverse growth-limiting environments[19,20] and organisms[7–9,21,22], most often manifesting as a linear correlation[1,2,8].

This tight coupling of population growth rate and ribosome levels has allowed important advances across diverse fields. It has enabled predicting the growth of cells from the levels of their ribosomes or other growth-supporting molecules[7,9,23,24], provided insights about the regulatory circuits that allow cells to fine-tune their growth to match their environments[16,19,25], and suggested trends governing how cells across the tree of life should evolve to optimize ribosome utilization[1,2,26,27]. More generally speaking, the idea that cells optimize their transcriptome and proteome to maximize their "cellular economy" has been a guiding principle across diverse biological disciplines[3,4,11].

Although literature pertaining to the growth law discusses the ribosomal content "per cell" and models how single cells regulate their ribosome content[1,2,8,25], the relationship between ribosomes and growth rate has most often been studied in aggregate. It has historically been difficult to measure the number of ribosomes in a single, tiny microbial cell. Alternatively, there are several well-established ways to macerate a large number of cells, measure the total amount of ribosome content in their lysate, typically as a mass-to-mass ratio of RNA to protein, and how that quantity changes across similarly sized populations of cells growing at different rates. Numerous studies following this approach have shown that a population's average ribosome level changes in lock step with its growth rate. But taking the average can mask heterogeneity[28]. For example, this may obscure subpopulations of cells that follow different evolutionary strategies to maximize fitness, such as cells that maintain high levels of ribosomes despite growing slowly[29,30]. This in turn may blind us to the existence of alternate regulatory circuits that allocate resources in different ways in certain cell populations or environments. These circuits may represent different evolutionary solutions to the problem of maximizing fitness given resource availability. In sum, perhaps we are missing interesting biology by averaging away these signals.

Here we investigate heterogeneity in ribosome levels across single cells by utilizing data we and others recently generated by using a novel high-throughput method (Split Pool Ligation based Transcriptome sequencing, SPLiT-seq) that enables the sequencing of transcriptomes of

individual microbial cells[31,32]. While more common cell isolation-based approaches have difficulty sequencing microbial cells due to their small size and unique anatomies, SPLiT-seq overcomes these limitations and allows capture of thousands of RNA transcripts per microbial cell[31,32]. We implemented SPLiT-seq using random hexamer primers that recover rRNA, in addition to the typically used polydT primers that bias recovery towards mRNA. This enables us to use these data to study how the ribosomal abundance of microbial cells changes as growth rate changes. We used data surveying roughly 8,200 haploid and diploid yeast cells (*Saccharomyces cerevisiae*) and 5,300 bacterial cells (*Bacillus subtilis*), sampled at different times – and thus varying growth rates – across the growth curve (**Figure 1a**). The cells averaged 6,390 or 2,644 rRNA reads per cell (for yeast and bacteria respectively).

Contrary to the expectation that cells optimize their ribosome content to match their growth rate, we find enormous heterogeneity in single-cell ribosome levels across genetically identical cells that have the same access to growth-supporting nutrients. When we focus on nutrient conditions supporting fast growth, cells do not exclusively have high ribosomal content or other transcriptional signatures of fast growth. Similarly, when we focus on only those cells with the most ribosomes, these cells do not exclusively possess transcriptional signatures of fast growth. Indeed, some show transcriptional signatures of stress. We conclude that, while the ribosomal content of cell populations is a strong predictor of population growth rate[7,9,23,24], the ribosomal content of a single cell appears to be a poor predictor. These results call for further study of the growth law, in particular, reconciliation of ideas about optimization of the cellular economy with data from single-cell studies revealing widespread heterogeneity.

RESULTS

Single-cell ribosome levels do not correlate with population growth rate. Either yeast (*S. cerevisiae*)[31] or bacteria (*B. subtilis*)[32] were grown in batch culture and sampled over time starting when populations were at or near steady state growth and ending as the cells were exhausting their nutrients (4 samples over time for yeast, 8 for bacteria). For each sample, cell counts or optical density were measured to create growth curves for each population of cells (**Figure 1a,** gray lines). To track the rate at which the populations of cells were growing at each time point, we calculated a sigmoidal function to fit the growth curve and then took the log2 ratio between the adjacent data points (**Figure 1a,** black lines). We used these calculations to estimate the instantaneous growth rate of each population we study in doublings or generations per hour (**Figure 1b-c,** horizontal axes). These cells sampled at each time point were also used to perform single-cell RNA sequencing via Split-Pool Ligation based transcriptomics sequencing (SPLiT-seq)[31,32]. We used these transcriptional data to calculate the ribosomal content of, on average, 2,045 and 683 single cells per sample for yeast and bacteria, respectively (**Figure 1b,** vertical axes). As expected, based on the growth law, there is a strong correlation between the average amount of ribosomal RNA in a population of cells and that population's instantaneous growth rate (**Figure 1b**). In both yeast and bacteria, we find that population growth rate explains 94% and 69% of variance in average rRNA abundance respectively when using a linear model (**Figure 1b,** R-

squareds). The non-linearity in slow-growing *B. subtilis* populations, in which ribosomal content appears to be less responsive to changes in nutrient content, has been observed for other bacterial species as well[22].

However, this correlation breaks down at the single-cell level where the population growth rate explains 5% and 12% of variance in single-cell rRNA abundance in yeast and bacteria respectively (**Figure 1c,** R-squareds). Even in conditions when cells are flush with nutrients and the population is doubling at the fastest rate we survey, there is massive variation in ribosome content across cells spanning more than two orders of magnitude (**Figure 1c**). Within a single timepoint, there is up to 25 times as much variation as we observe on average across timepoints (**Figure 1b**). The high level of variation we observe seems unexpected if single cells optimize their ribosome levels to maximize their growth rate given the nutrient availability.

We ruled out several obvious explanations for this heterogeneity. First, we asked if variation may represent measurement noise. If most of the variation is resultant from sampling noise, then we would expect relative noise to be highest in slow-growing populations of cells that have, on average, fewer ribosomal transcripts. However, that is not the case (**Figures 1 & 2**). Second, we explored whether other measures of single-cell ribosomal content might be a better predictor of the population's growth rate and nutrient access. For example, normalizing each cell's rRNA content by its mRNA content may serve as a general estimate for the portion of each cell's ribosomes that are active, which recent work shows also correlates with growth rate[33,34]. mRNA is a highly transient molecule in microbes and should be readily occupied by ribosomes[35,36]. If the mRNA/rRNA ratio is high, we expect that the cell is metabolically active, since it is dedicating more of its transcriptional energy to mRNA. We also expect that the ribosomes should be actively translating those molecules given their short half-life. In support of our intuition, in both yeast and bacteria, we see the same strong correlation between the population's average mRNA/rRNA ratio and the population's growth rate that is expected given the growth law (**Figure S1a**-i; population growth rate explains 69% and 83% of variance in mRNA/rRNA ratio, respectively). But just as we observe for the rRNA abundance, the correlation with growth rate becomes much weaker at the single-cell level (**Figure S1b**-i; population growth rate explains 9% and 5% of variation in mRNA/rRNA ratio respectively). Similar results are observed when looking at log-normalized and scaled scRNAseq counts (**Figure S1a,b**-ii) and ribosomal protein mRNAs (**Figure S1a,b**-iii). Third, variation in absolute rRNA counts could reflect differences in cell size. However, the normalization methods above, such as the ratio of mRNA/rRNA, are independent of cell size. Further, our analysis includes both haploid and diploid strains of yeast, which are known to differ in size by approximately 1.5X on average[37]. And yet, ploidy explains less than 1% of the variance in single-cell rRNA abundance (**Figure S2**). Finally, variation in predicted cell cycle state[38] also does not explain the heterogeneity we observe in the yeast data (**Figure S3**). This is consistent with other work suggesting that ribosome levels do not fluctuate with the cell cycle[7,11]. Given none of these hypotheses explain the variation in single-cell ribosomal content that we observe, we next explored if heterogeneity in single-cell ribosomal content simply reflects heterogeneity in single-cell growth rates.

Single-cell growth rate heterogeneity does not explain heterogeneity in rRNA abundance. One hypothesis to explain the large variation in single-cell rRNA abundance is that it is due to corresponding heterogeneity in single-cell growth rates. In some ways, this hypothesis is consistent with the growth law because it asserts that every single cell's ribosome content is tightly correlated to its own rate of growth. If this were true, then single-cell growth rates should be most heterogeneous when single-cell ribosome abundances are also most variable. Interestingly, we observe that rRNA abundance heterogeneity (as calculated by the mean normalized standard deviation, or coefficient of variation σ/μ) correlates positively to the population's growth rate. That is to say, fast growing populations of cells sampled when nutrients are most abundant have the highest heterogeneity in rRNA counts in both yeast and bacteria (**Figure 2a**). This positive correlation between ribosome heterogeneity and population growth rate appears to be consistent with at least one previous study in another organism[22]. This trend persisted for another measure of data variance or spread (**Figure S4**). To understand whether heterogeneity in ribosomal content reflects heterogeneity in single-cell growth rates, we sought to find if heterogeneity in single-cell growth rates is positively correlated with the population growth rate.

Here, we investigate how heterogeneity in single-cell growth rates varies with population growth rate using two different approaches. First, we infer single-cell growth rates from gene expression profiles, or the genes and quantities of expression detected in each cell. Previous work reports correlation values between gene expression and growth rate for the majority of *S. cerevisiae* genes[9,23]. Genes for which expression is higher during faster growth have positive correlation values, and those for which expression is higher during slow growth have negative correlations. We used the associative values in Brauer et al. 2008[9] to weight the gene expression in our single cells and calculate an arbitrary predicted growth rate (**Figure S5a**) using the formula described in the Methods.

Next, we used these inferred values to ask if variation in single-cell growth rates positively correlates with the population growth rate, as does variation in single-cell ribosome levels (**Figure 2b**). To do so, we took the coefficient of variation of the predicted single-cell growth rates for each population growth rate as a measure of growth rate heterogeneity. However, unlike the rRNA abundance heterogeneity (**Figure 2a**), the heterogeneity in single-cell growth rate negatively correlates with population growth rate in yeast. This may suggest that variation in the growth of individual cells is not responsible for the spread of rRNA abundance we observe. Additionally, comparing the rRNA/cell to the inferred single-cell growth rates explained less than 1% of the variance observed (**Figure S5b**).

However, these measurements may suffer from the same issue we observe in rRNA abundance–that is, they were estimated using values taken from the mean of a bulk population. Thus, we also performed a second analysis to confirm our results that does not rely on inference from scRNAseq data. For this analysis, we used an independent data set of single-cell *S. cerevisiae* growth measurements where the growth of thousands of yeast microcolonies was monitored over time using high-throughput microscopy[39]. We aggregated all microcolonies and averaged the

growth rate for each timepoint to generate a proxy for population growth rate. Like our data, the mean growth rate generally decreases with time as nutrients are consumed. We then again calculated the heterogeneity using the coefficient of variation of the individual growth rates of the microcolonies as stratified by time point. Like our gene expression predicted growth rate data, the heterogeneity of single-cell growth rates declines as the population average increases (**Figure 2c**). These negative correlations are the opposite of what we see in the rRNA data.

In sum, we show that single-cell growth rates are most heterogeneous in slow-growing populations of cells (**Figure 2b-c**), but single-cell ribosome levels are most heterogeneous in fast-growing populations of cells (**Figure 2a**). These results, and others[40], do not support the hypothesis that single-cell growth rate variation is driving the heterogeneity we observe in rRNA abundance. Next, we further analyzed the heterogeneity in single-cell ribosomal content by using data from the rest of the transcriptome.

Transcriptional analysis reveals heterogeneous cell types even within steady-state growth. Heterogeneity in and of itself seems potentially inconsistent with the spirit of the growth law, which is based on the idea that cells have evolved to tightly optimize their cellular economy[3,4,11]. We were particularly surprised to see high heterogeneity in single-cell ribosome levels in our fastest growing populations of cells because these populations were collected at or near steady-state growth. Previous works demonstrating ribosomal growth laws are often performed on populations of cells growing at steady state[9,15,16,25]. These studies make the implicit assumption that steady-state populations are homogeneous such that it is possible to model the number of ribosomes (or other molecules) per cell from population-level measurements[25]. This assumption is consistent with a model in which cells are all similarly striving to optimize their levels of ribosomes to match the maximum growth rate supported by the nutrient concentration. However, it is within our steady-state timepoints that we paradoxically observe the most rRNA abundance variability. Therefore, we examined the rest of the transcriptome in these fastest growing populations of cells to understand to the extent their other behaviors support or contradict this supposition of uniformity.

Contrary to expectations, there are variant expression patterns between cells when our populations are in, or close to, steady state (**Figure 3**). In both yeast and bacteria, we observe cells that show the expression signatures associated with faster growth–genes related to ribosome production, translation, carbon utilization, RNA processing, and cell replication. However, we also find cells that show signs of classic stress responses–general stress proteins, genes related to respiration and the TCA cycle and mitochondrial proteins, trehalose metabolism[41], and low glucose conditions (**Figure 3**). We wondered if perhaps the cells expressing stress-related transcripts represent those that are growing slower due to stressors like DNA damage or cell aging. However, when we compare the cells mounting a transcriptional response characteristic of "growth" vs. "stress", we see a near complete overlap between the distributions of ribosome abundance (**Figure 3**). This observation adds further support to our burgeoning conclusion that it

is difficult to predict the growth rate of single cells from rRNA levels or the levels of other transcripts.

Perhaps one explanation for these data is that even our earliest sampled cell populations are not actually in steady state growth, despite having been previously grown at low density for multiple generations in rich media before being transferred into fresh and ample nutrients for the reported growth curves. However, given heterogeneity in ribosome levels increases as we sample closer to steady state (**Figure 2a**), it seems unreasonable to suggest that these diverse transcriptional signatures would disappear had we sampled cells closer to steady state growth. Further, it is important to study the degree to which growth laws break down in environments that are commonly encountered in nature, such as those where nutrient levels are decreasing over time[42]. Indeed, the diverse transcriptional signatures we observe are not restricted to cells growing at or near steady state. Cells expressing growth-responsive and cells expressing stress-responsive transcripts are present in multiple timepoints along the growth curve (**Figure S6**). Given these two cell types have largely overlapping ribosomal contents (**Figure 3**), it appears difficult to predict an individual cell's growth behavior from its ribosome level, regardless of whether cell populations are growing at or near steady-state or not.

The heterogeneity we observe is consistent with other studies that show single-cell heterogeneity is the rule rather than the exception[28,32,39,41,43,44]. Though high-throughput single-cell transcriptomics in microbial cells is just emerging, previous work examining the transcriptomes of a small number of cells or higher-throughput studies using fluorescent markers have shown that heterogeneity is incredibly common. For example, previous work suggests that persister cells[45,46], or more generally, slow growing cells that have unusually high stress tolerance[41], exist even in fast-growing cell populations that have access to high levels of nutrients. Even under conditions of stress, when mounting a transcriptional stress response may mean the difference between life or death, not all cells respond uniformly, or even respond at all[47,48].

Single-cell heterogeneity sometimes reflects bet-hedging, in other words, a simultaneous display of multiple evolutionary strategies to prepare for an unknown future[41,49]. For example, an alternate evolutionary strategy, besides maximizing growth rate, may involve harboring excess ribosomes to prepare for conditions that require increased translation[29,42,50,51]. Another strategy may involve expressing stress-responsive, rather than growth-responsive transcripts, to prepare for unexpected and unfavorable environments[41,45,46]. But cell-to-cell heterogeneity could also simply result from unavoidable processes like expression stochasticity, DNA damage, or aging[44,52,53]. Whatever the underlying cause of the heterogeneity, our observation that all single cells do not seem to optimize their ribosome content (or their transcriptomes) to match their nutrient level may call for additional work reconciling the growth law with single-cell heterogeneity and the knowledge that cells can maximize fitness via diverse evolutionary strategies.

Cells with the most ribosomes do not all have transcriptional signatures of faster growth, and cells with the fewest ribosomes do not all have signatures of slower growth. To further investigate whether the ribosomal content of a cell is optimized to match its rate of growth,

we decided to compare "apples to apples," so to speak. We ordered the cells by their ribosome abundance from least to greatest across all time points. If ribosomes are the dominant signatures of growth rate, we would expect the cells with the most ribosomes to have uniform growth signals in their transcriptomes, and the cells with the least ribosome abundance to show signs of stress or slow growth.

We separated the cells into four quartiles and used Louvain clustering to investigate any subpopulations that might be present within each quartile. Differential expression analysis on the identified subpopulations revealed that, within each quartile, cells segregated by signatures of growth and stress (**Figure 4a**). Contrary to our expectations given the growth law, the cells with the highest number of rRNAs do not all have transcriptomes suggestive of fast growth (**Figure 4a,** i-ii). Similarly unexpected under the assumptions of the growth law was that some cells with the fewest ribosomes still appear to be employing transcriptional programs associated with a growth-oriented directive (**Figure 4a,** iii-iv).

In yeast, the "growth" clusters (**Figure 4a;** green) are defined by the expression of genes involved in glycolysis, ribosome biogenesis, and translation. The "stress" clusters (**Figure 4a,** gray) show upregulated gene expression of heat stress, osmotic stress, and protein misfolding stress pathways. In bacteria, in the "growth" clusters (**Figure 4a,** green) we see differential expression of similar translation and ribosome biogenesis pathways, and also operons involved in the import and digestion of preferred carbon sources. The "stress" cluster (**Figure 4a,** gray) is defined by expression of genes such as sporulation initiation, bacteriocin production, and surfactin production. Additionally, in both organisms we see an intermediate cluster of cells (**Figure 4a,** light green) that are shifting from glycolysis and preferred carbon digestion to the TCA cycle and operons for the import and digestion of less desirable carbon sources such as short chain fatty acids, and in *B. subtilis*, the lichenan pathway[54]. The salient observation is that all clusters (stress and growth) are present in all quartiles, including those containing cells with the most ribosomes (**Figure 4a,** i-ii) and cells with the least ribosomes (**Figure 4a,** iii-iv). This suggests that each single cell's ribosome content is not tightly optimized to match the maximum growth rate supported by its environment.

An alternate interpretation of the growth law might posit that cells with the highest or the lowest ribosome content include those with non-optimal numbers of ribosomes given their environment. In this case, one might expect cells that have an intermediate ribosomal content to express growth-responsive, rather than stress-responsive transcripts. However, this interpretation is inconsistent with our observation that both cell types (those expressing growth-responsive or stress-responsive transcripts) are present in quartiles of cells possessing intermediate amounts of ribosomes as well. Further even after we sort by ribosome abundance, the strongest signature in the clustering is the sample time point (**Figure 4b**). This suggests that a cell in a quartile of ribosomes from early in the growth curve and a cell with comparable ribosomes from later on are not most essentially defined by their ribosome abundance. Perhaps this result appears obvious in retrospect, but if ribosomes and growth activities were intrinsically linked as the growth law suggests, then the null assumption would be that these cells should be alike. Seemingly, having

similar amounts of rRNA does not make cells similar at the rest of the transcriptional level. Overall, our findings advise caution when equating an individual cell's ribosome level to its growth rate, or more generally, to any particular cell state or behavior.

DISCUSSION

How does something so noisy, like the ribosomal content of single cells, underlie something so predictable, like a relationship describing how the ribosomal content of a cell population changes with nutrient availability? This question pertains not only to the growth law studied here, but more broadly as well, given that transcription is inherently noisy[44] yet many cellular behaviors are predictable[54]. One hypothesis as to why we observe so much variation in rRNA levels is that transcription of rRNA involves large bursts followed by long periods at a steady state level set by the environment, which recent work has shown is the case for ribosomal protein mRNA[55,56]. If such bursts of rRNA transcription can become asynchronous, occurring in different cells at different times, it could explain some of the heterogeneity in rRNA content that we see. However, this hypothesis cannot account for all the heterogeneity if different cell types have different bursting behavior or are set to different steady-state rRNA levels. Indeed, we see evidence that different types of cells exist simultaneously, including cells that are expressing growth-related vs. stress-related transcripts (**Figure 3**), cells that express a high abundance of retrotransposons (**Figure 5A**), and cells that appear to be sporulating even when nutrients are abundant (**Figure 5B**). The spores are particularly curious as they occur in every time point sampled from only one of two replicate experiments. This discrepancy between replicates is consistent with previous work demonstrating that cell growth is sensitive to minute differences between ostensibly identical experiments[57–59]. The sensitivity of cells to small environmental changes, combined with the heterogeneity in cell types that exists even when nutrients abound, highlights the incredible diversity of cell behavior and the lingering mysteries surrounding how cells regulate that behavior in response to environmental stimuli.

METHODS

Growth curve and single-cell sequencing data. Cell culture methods were described in previously published works by L. Brettner and others[31,32]. Briefly, overnight liquid cultures from colonies of diploid s288c cells and haploid BY4741 *Saccharomyces cerevisiae* and PY79 *Bacillus subtilis* cells were started in cultures of ~300 cells/mL in synthetic complete plus 2% glucose media for yeast or OD600 0.02 in Lennox broth media for bacteria respectively. These cultures were then sampled and measured systematically until the populations started to enter stationary phase. The samples were saved and processed for single-cell RNA sequencing using the SPLiT-seq method[31,32,60]. Sequencing data for these experiments have also already been published[31,32]. However, the saved *S. cerevisiae* sample libraries were re-sequenced on the NovaSeqX platform with paired end reads for a total of 300 cycles. This provided further and deeper coverage than

what was reported in Brettner et al. 2024[31]. Sequencing and processed data for *S. cerevisiae* can be found through GEO at accession number GSE251966 and for *B. subtilis* at GSE151940. Additional processed data and analysis scripts can be found at the Open Science Framework: https://osf.io/kjfbz/. Additionally, there were two repeat experiments reported in Kuchina and Brettner et al. 2021[32], described as M14 and M15. We focus most of our analyses on the data from M15 as the data in M14 suggest many of the cells may be transitioning to a non-growing sporulation state (**Figure 5b**).

Cell density curve and growth rate curve calculations. The cell densities reported in cells/mL for yeast and OD600 for bacteria, and timepoints in hours were used to calculate a sigmoidal curve through a nonlinear weighted least-squares estimate in R (nls function). The model was fitted to the function for a sigmoid as follows (**Figure 1a,** gray lines).

$$cell\ density = \frac{L}{1 + e^{-k(t-t_0)}}$$

Where L is the saturation density, t0 is the half maximal time, and k is the slope. The data points from these models were then used to fit the growth rate curve in generations per hour using a log2 ratio between adjacent points normalized to the time increment as follows (**Figure 1A,** black lines).

$$\frac{generations}{hr} = \log_2 \frac{\left(\frac{cell\ density[i]}{cell\ density[i-1]}\right)}{\Delta t}$$

A sigmoidal function might not be the best approximation of growth under very low densities and early in the growth curve as it assumes continuous exponential growth and cannot incorporate any kind of lag phase. This might explain why the maximal estimated yeast growth rate is slightly higher than typically reported in the literature (~1.05 generations/hour compared to ~0.75 generations/hour). However, the absolute value is of little importance, and instead the shape of the curve and the relative relationships between the points are what impact the relevant downstream models (eg. the goodness of linear fits, R^2).

Single-cell RNA seq data processing, rRNA abundance calculations, and mRNA normalization. Sequencing reads were aligned to the R64 s288c genome for *Saccharomyces cerevisiae* from NCBI or the ASM904v1.45 genome for *Bacillus subtilis* from EnsemblBacteria and sorted by barcode using STARsolo[61]. As both the yeast and bacterial genomes have significant sequence homology, especially within rRNA genes, we enabled the uniform multimapping algorithm within STARsolo to keep overlapping reads. This outputted gene-by-barcode matrices representing the detected gene counts for every cell. To remove empty and low gene detection barcodes, we applied the "knee" detection filter previously described in Brettner et al. 2024[31]. These quality-thresholded gene-by-barcode matrices were then converted to the R datatype, Seurat Objects, using the Seurat R package for further analyses[62].

rRNA genes were identified using the Saccharomyces Genome Database (SGD)[63] and SubtiWiki[64]. Counts from these genes were then aggregated to calculate an rRNA abundance for each cell. While single-cell RNA sequencing data is typically highly sparse for mRNA, the

minimum combined rRNA counts detected in one cell in these data were well above 500 reads. As scRNAseq data normalization methods are designed for sparse, low count data, we used the raw total rRNA counts in all ribosome abundance analyses to avoid unnecessary data distortion[65].

Normalization, scaling, nearest neighbor calculations, clustering, and differential expression analyses were performed similar to the tutorial provided by the Satija Lab[66] on mRNA datasets with the rRNA removed. As rRNA typically makes up greater than 90% of the detected RNA reads and clustering is relative, keeping it in made for skewed clustering analyses that obscured some of the interesting biological behaviors.

Estimating single-cell growth rates from transcriptional data. Gene expression and growth rate correlation values were obtained from Brauer et al. 2008[9]. These values were used to weight normalized and scaled mRNA expression for each cell using the following formula with rRNA genes removed.

$$single\ cell\ estimated\ growth\ rate = \frac{\sum_{i}^{all\ genes} Brauer\ correlation_i * gene\ expression_i}{total\ detected\ expression}$$

This equation produces an arbitrary, unitless number. The more positive the number, the more the transcriptome of that cell is indicative of growth-related expression and vice versa.

Within timepoint analyses (Figure 3). We bioinformatically separated out the transcriptomes of the exponentially growing cells from the sample timepoints that best approximate steady-state growth (**Figure 1a**). These also happen to be the timepoints with the highest mean rRNA abundance and the most recovered cells. In yeast, this sample corresponds to the first timepoint when the cells are at $9.2*10^6$ cells/mL and growing at an estimated 1.05 generations/hour. In bacteria, we chose the timepoint when the cells were at OD600 of 1.0 and a growth rate of 1.22 generations/hour. This corresponds to the second timepoint in the bacterial series, but the difference in growth rate from the first timepoint at OD600 0.5 is only approximately -0.03 generations per hour. More importantly, this second timepoint has almost 2.5 times more recovered cells, significantly increasing the resolution of any subpopulations detected via clustering methods. Additionally, this second timepoint also has the highest mean rRNA abundance.

We then applied a Louvain clustering algorithm to these cells with a low enough resolution to only produce 2 to 3 clusters. We then performed a differential expression analysis on these clusters and categorized the top 20 positive genes in each using SGD[63], Metascape[67], or SubtiWiki[64]. We used these categorizations to classify each cluster, and found they dichotomized by growth and stress related genes. We sorted out the cells by barcode for each cluster and used violine plots to visually compare the rRNA means and distributions.

"Apples to apples" rRNA quartile analyses (Figure 4). We first calculated the minimum and maximum rRNA abundances for each timepoint and found the largest minimum and smallest maximum. The largest minimum and smallest maximum were used to create a bandwidth filter to allow for more direct comparisons of cells with similar rRNA amounts with representatives from

each timepoint. Cells within this bandwidth were sorted by rRNA from least to greatest and quartiles were calculated. We then applied the same Louvain clustering to cells from each quartile and analyzed the gene categorizations and ontologies as above.

FIGURES

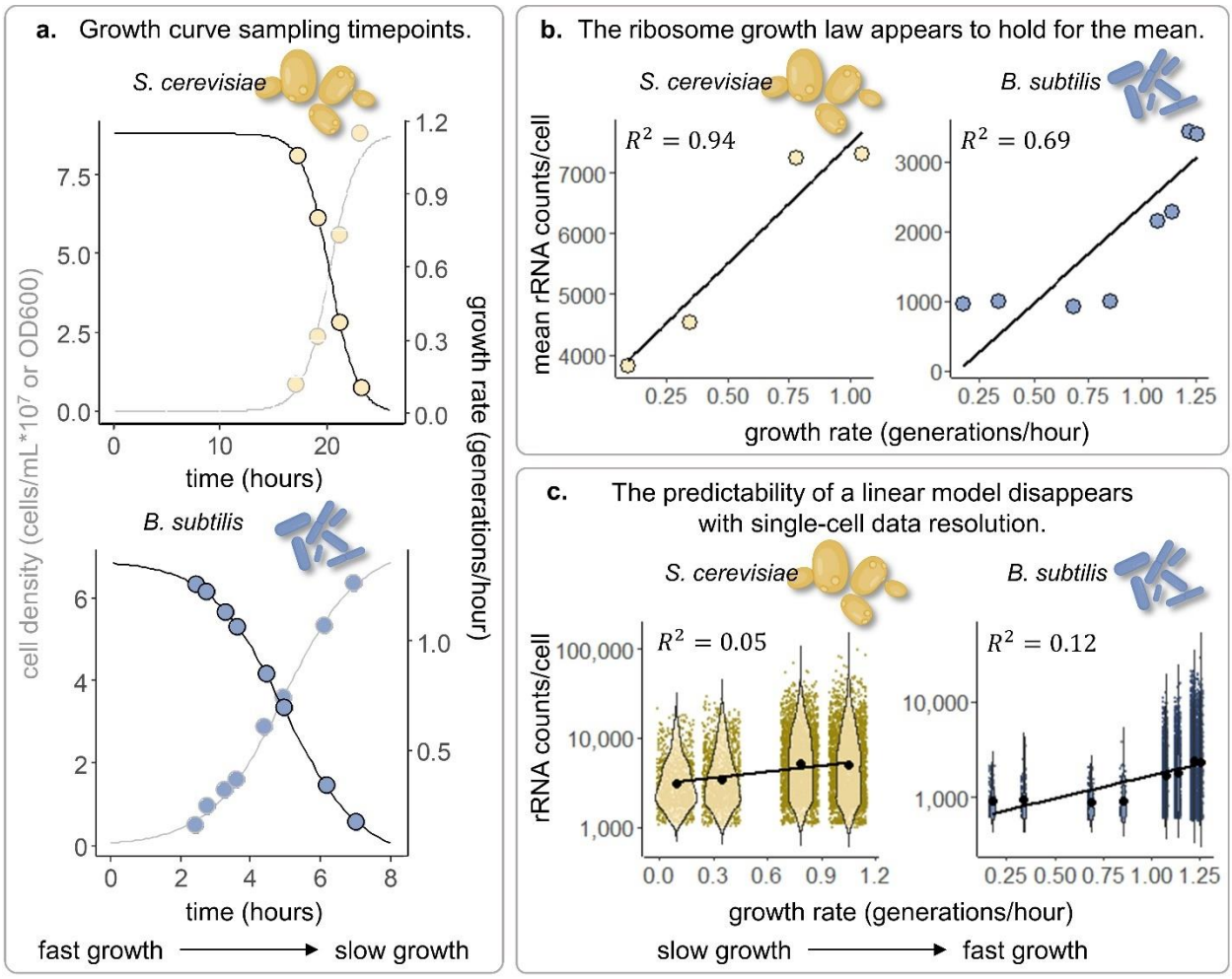

Figure 1. Population average ribosome levels correlate with population growth rates, but single-cell ribosome levels do not. a.) Cell density (black) given in cells/mL*10^7 in yeast and OD600 in bacteria and growth rate in generations per hour (gray) against time in hours. Yeast were sampled at 0.92, 2.7, 5.7, and 8.6*10^7 cells per milliliter. Bacteria were sampled at OD600 0.5, 1.0, 1.3, 1.6, 2.0, 3.6, 5.3, and 6.0. Yeast and bacteria cartoon icons were created using Biorender[68]. **b.)** mean detected rRNA counts per cell versus the population growth rate in generations per hour. Trend lines and R^2s were calculated by applying a linear regression model to the mean data points in R. **c.)** rRNA counts for all datapoints represented as violin distributions. Means (black dots) and trendlines are the same as in b. R^2s were calculated by applying a linear regression model to the entire dataset.

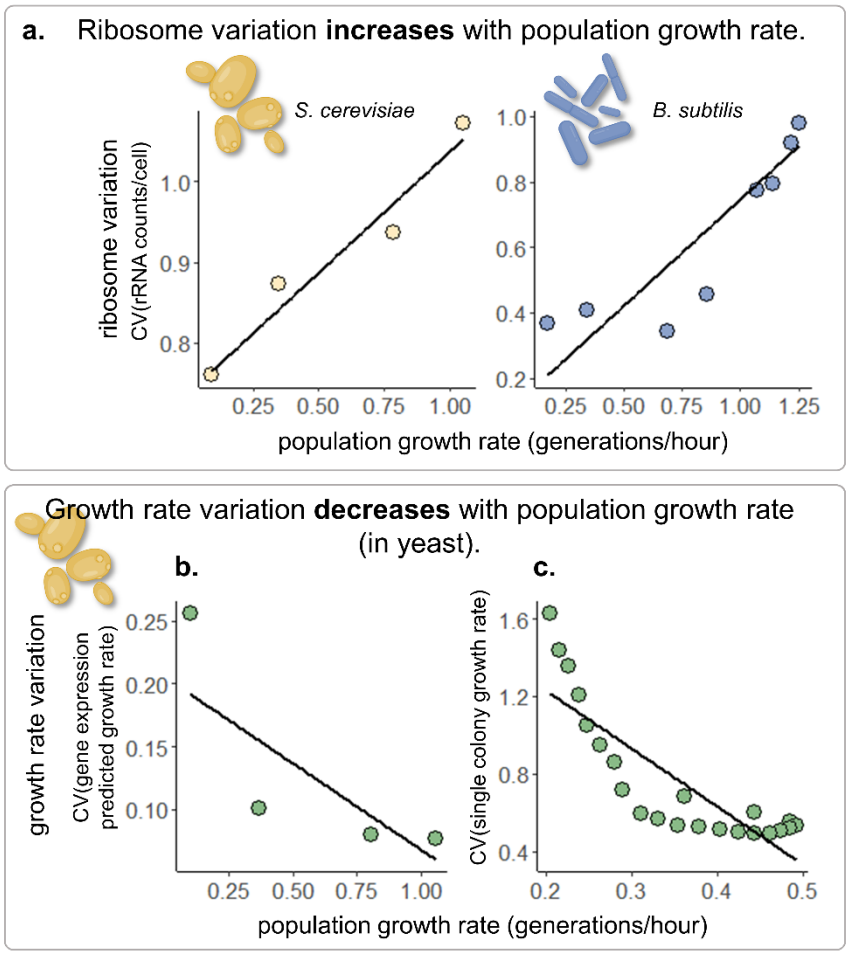

Figure 2. Single-cell ribosome heterogeneity trends opposite to single-cell growth rate heterogeneity. a.) Coefficient of variation (σ/μ) of ribosome counts for cells in each timepoint against population growth rate. **b.)** Coefficient of variation of single-cell growth rates estimated using gene expression (Methods) for cells in each timepoint against population growth rate. **c.)** Coefficient of variation of single microcolony growth rates against the average growth rate for each imaging time[39]. Trendlines are shown to indicate the direction of correlation with population growth rate.

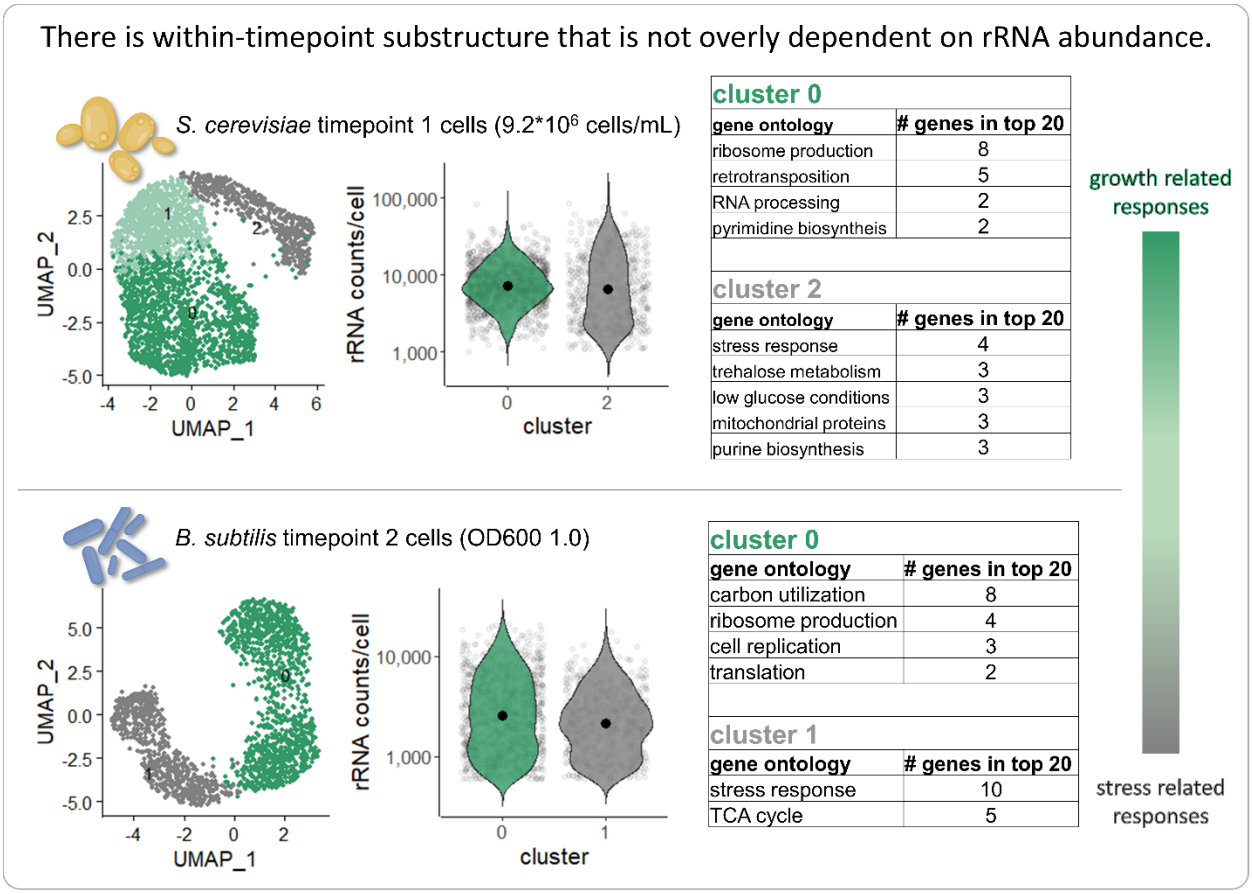

Figure 3. UMAP embeddings for cells from the first timepoint in yeast ($9.2*10^6$ cells/mL) and second timepoint in bacteria (OD600 1.0) colored by Louvain cluster. Ribosome counts per cell distributions for growth gene expression dominated (green) and stress gene expression dominated (gray) clusters. Gene ontologies for the top 20 differentially expressed genes in each cluster that appear for two or more genes.

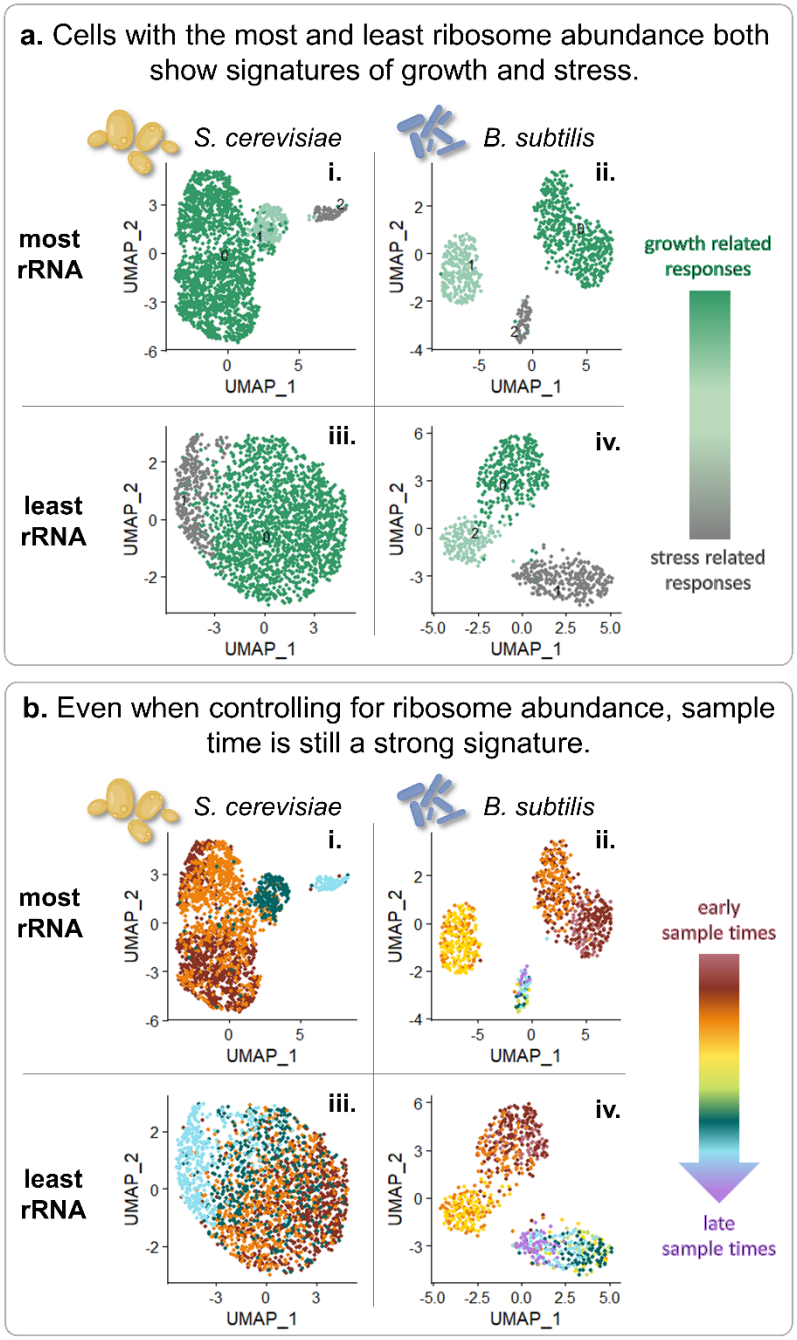

Figure 4. Cells show differential subpopulations and signatures of sample timepoint despite having similar ribosome levels a.) UMAP embeddings of cells from the most (i-ii) and least (iii-iv) rRNA abundance quartiles colored by Louvain cluster. **b.)** UMAP embeddings of cells from the most (i-ii) and least (iii-iv) rRNA abundance colored by sample timepoint.

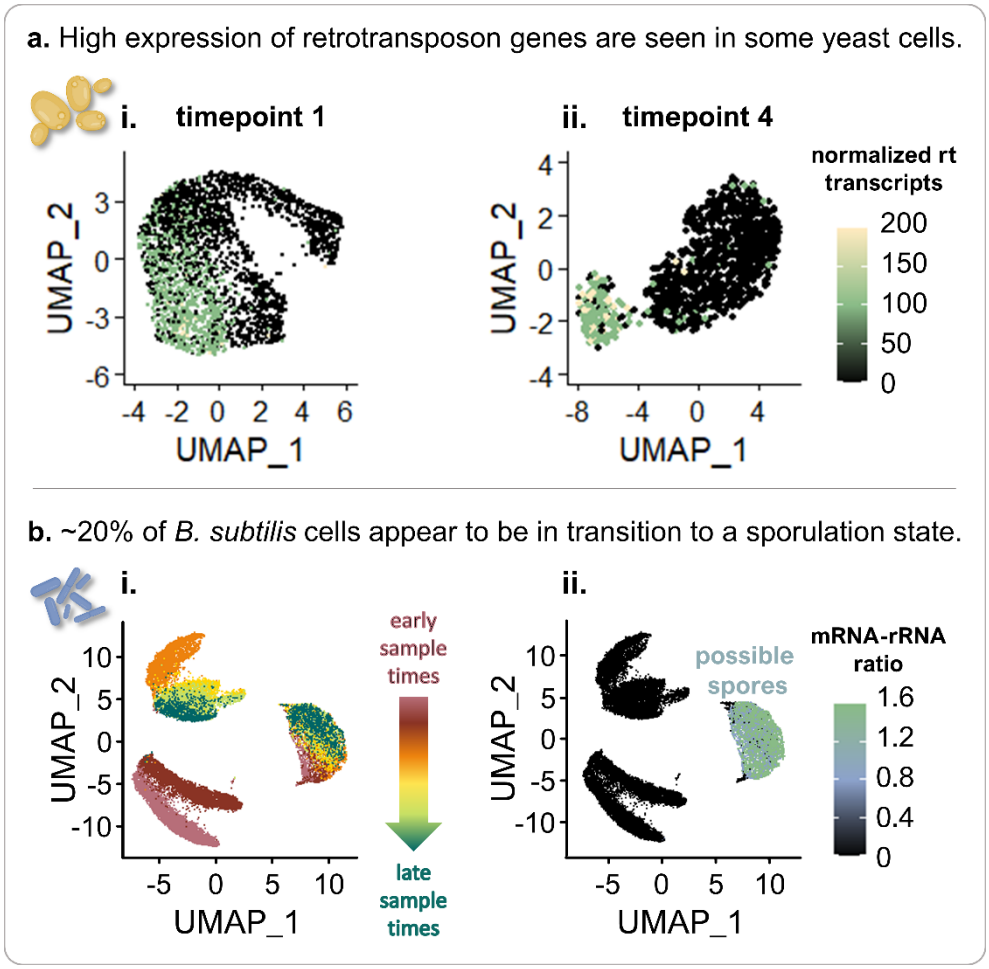

Figure 5. Unexpected subpopulations are observed across the growth curve in both yeast and bacteria a.) UMAP embeddings of cells from the first timepoint (i) and the last timepoint (ii) of the yeast growth curve colored by retrotransposon gene transcript abundance. Retrotransposons are mobile genetic elements within the yeast genome typically thought to be activated by stress[69]. However, here we strangely observe them in not only in a subpopulation of cells in the final timepoint of the yeast growth curve, but also in the first timepoint in cells with transcriptional signatures of fast growth (**Figure 3**). **b.)** UMAP embeddings of bacterial cells from an independent replicate experiment in Kuchina and Brettner et al. 2021[32] colored by sample time (i) or mRNA-rRNA ratio (ii). We excluded this replicate from our analysis because we noticed that it appears to contain sporulating cells. This was first revealed by a bimodal distribution of mRNA-rRNA ratios, where a subpopulation ranging from 16% to 50% of cells, depending on the timepoint, appeared to have a very high ratio of mRNA to rRNA. Upon performing a differential expression analysis, we observed that over 30% of the top 100 upregulated genes in these subpopulations were related to sporulation, leading us to believe these cells might be in transition to a non-growing sporulation state despite being grown in rich media. Sample times in (i) correspond to 6 timepoints ranging from OD600 0.5 to 3.2.

ACKNOWLEDGEMENTS

Funding for this work was provided by a National Institutes of Health grant R35GM133674 (to KGS), an Alfred P Sloan Research Fellowship in Computational and Molecular Evolutionary Biology grant FG-2021-15705 (to KGS), and a National Science Foundation Biological Integration Institution grant 2119963 (to KGS). We would also like to thank Michael Lynch for helpful conversations, and the members of the ASU Biodesign Center for mechanisms of Evolution and the Geiler-Samerotte Lab for their support and feedback.

AUTHOR CONTRIBUTIONS

LB and KGS conceived of the study and contributed to writing the manuscript. LB performed the experiments and analyses.

REFERENCES

1. Lynch, M. Evolutionary Scaling Laws in Cell Biology. in *Evolutionary Cell Biology: The Origins of Cellular Architecture* (2022).
2. Lynch, M. Cell Growth and Division. in *Evolutionary Cell Biology: The Origins of Cellular Architecture* (2023).
3. Golan, O. *et al.* Models of growing cells. in *Economic Principles in Cell Biology* 117–134 (2024).
4. Kremling, A., Liebermeister, W., Noor, E. & Wortel, M. Metabolism in states of maximal enzyme efficiency. in *Economic Principles in Cell Biology* 107–116 (2024).
5. Schaechter, M., Maaloe, O. & Kjeldgaard, N. O. Dependency on medium and temperature of cell size and chemical composition during balanced grown of Salmonella typhimurium. *J Gen Microbiol* **19**, 592–606 (1958).
6. Scott, M. & Hwa, T. Bacterial growth laws and their applications. *Current Opinion in Biotechnology* **22**, 559–565 (2011).
7. Airoldi, E. M. *et al.* Predicting Cellular Growth from Gene Expression Signatures. *PLOS Computational Biology* **5**, e1000257 (2009).
8. Scott, M., Gunderson, C. W., Mateescu, E. M., Zhang, Z. & Hwa, T. Interdependence of Cell Growth and Gene Expression: Origins and Consequences. *Science* **330**, 1099–1102 (2010).
9. Brauer, M. J. *et al.* Coordination of growth rate, cell cycle, stress response, and metabolic activity in yeast. *Mol Biol Cell* **19**, 352–367 (2008).
10. Maaløe, O. Regulation of the Protein-Synthesizing Machinery—Ribosomes, tRNA, Factors, and So On. in *Biological Regulation and Development: Gene Expression* (ed. Goldberger, R. F.) 487–542 (Springer US, Boston, MA, 1979). doi:10.1007/978-1-4684-3417-0_12.

11. Warner, J. R. The economics of ribosome biosynthesis in yeast. *Trends Biochem Sci* **24**, 437–440 (1999).
12. Wilson, D. N. & Nierhaus, K. H. The Weird and Wonderful World of Bacterial Ribosome Regulation. *Critical Reviews in Biochemistry and Molecular Biology* **42**, 187–219 (2007).
13. Ali, A. *et al.* Adaptive preservation of orphan ribosomal proteins in chaperone-dispersed condensates. *Nat Cell Biol* **25**, 1691–1703 (2023).
14. Pelava, A., Schneider, C. & Watkins, N. J. The importance of ribosome production, and the 5S RNP–MDM2 pathway, in health and disease. *Biochem Soc Trans* **44**, 1086–1090 (2016).
15. Scott, M., Klumpp, S., Mateescu, E. M. & Hwa, T. Emergence of robust growth laws from optimal regulation of ribosome synthesis. *Mol Syst Biol* **10**, 747 (2014).
16. Bosdriesz, E., Molenaar, D., Teusink, B. & Bruggeman, F. J. How fast-growing bacteria robustly tune their ribosome concentration to approximate growth-rate maximization. *The FEBS Journal* **282**, 2029–2044 (2015).
17. Keren, L. *et al.* Promoters maintain their relative activity levels under different growth conditions. *Molecular Systems Biology* **9**, 701 (2013).
18. Gasch, A. P. *et al.* Genomic Expression Programs in the Response of Yeast Cells to Environmental Changes. *MBoC* **11**, 4241–4257 (2000).
19. Towbin, B. D. *et al.* Optimality and sub-optimality in a bacterial growth law. *Nat Commun* **8**, 14123 (2017).
20. Wang, Q. & Lin, J. Environment-specificity and universality of the microbial growth law. *Commun Biol* **5**, 1–9 (2022).
21. Zavřel, T. *et al.* Quantitative insights into the cyanobacterial cell economy. *eLife* **8**, e42508 (2019).
22. Matamouros, S. *et al.* Growth-rate dependency of ribosome abundance and translation elongation rate in Corynebacterium glutamicum differs from that in Escherichia coli. *Nat Commun* **14**, 5611 (2023).
23. Slavov, N. & Botstein, D. Coupling among growth rate response, metabolic cycle, and cell division cycle in yeast. *MBoC* **22**, 1997–2009 (2011).
24. Tadmor, A. D. & Tlusty, T. A Coarse-Grained Biophysical Model of E. coli and Its Application to Perturbation of the rRNA Operon Copy Number. *PLOS Computational Biology* **4**, e1000038 (2008).
25. Wu, C. *et al.* Cellular perception of growth rate and the mechanistic origin of bacterial growth law. *Proceedings of the National Academy of Sciences* **119**, e2201585119 (2022).
26. Maitra, A. & Dill, K. A. Bacterial growth laws reflect the evolutionary importance of energy efficiency. *Proceedings of the National Academy of Sciences* **112**, 406–411 (2015).
27. Bruggeman, F. J., Planqué, R., Molenaar, D. & Teusink, B. Searching for principles of microbial physiology. *FEMS Microbiology Reviews* **44**, 821–844 (2020).
28. Geiler-Samerotte, K. A. *et al.* Quantifying Condition-Dependent Intracellular Protein Levels Enables High-Precision Fitness Estimates. *PLOS ONE* **8**, e75320 (2013).

29. Metzl-Raz, E. *et al.* Principles of cellular resource allocation revealed by condition-dependent proteome profiling. *eLife* **6**, e28034 (2017).
30. Kafri, M., Metzl-Raz, E., Jonas, F. & Barkai, N. Rethinking cell growth models. *FEMS Yeast Research* **16**, fow081 (2016).
31. Brettner, L., Eder, R., Schmidlin, K. & Geiler-Samerotte, K. An ultra high-throughput, massively multiplexable, single-cell RNA-seq platform in yeasts. *Yeast* **41**, 242–255 (2024).
32. Kuchina, A. *et al.* Microbial single-cell RNA sequencing by split-pool barcoding. *Science* **371**, (2021).
33. Calabrese, L., Ciandrini, L. & Cosentino Lagomarsino, M. How total mRNA influences cell growth. *Proceedings of the National Academy of Sciences* **121**, e2400679121 (2024).
34. Dai, X. *et al.* Reduction of translating ribosomes enables Escherichia coli to maintain elongation rates during slow growth. *Nat Microbiol* **2**, 16231 (2016).
35. Petersen, N. S., Mclaughlin, C. S. & Nierlich, D. P. Half life of yeast messenger RNA. *Nature* **260**, 70–72 (1976).
36. Rauhut, R. & Klug, G. mRNA degradation in bacteria. *FEMS Microbiology Reviews* **23**, 353–370 (1999).
37. Sherman, F. Getting started with yeast. *Methods Enzymol* **350**, 3–41 (2002).
38. Spellman, P. T. *et al.* Comprehensive Identification of Cell Cycle–regulated Genes of the Yeast Saccharomyces cerevisiae by Microarray Hybridization. *Molecular Biology of the Cell* **9**, 3273 (1998).
39. Ziv, N., Siegal, M. L. & Gresham, D. Genetic and Nongenetic Determinants of Cell Growth Variation Assessed by High-Throughput Microscopy. *Mol Biol Evol* **30**, 2568–2578 (2013).
40. Pavlou, A. *et al.* Single-cell data reveal heterogeneity of resource allocation across a bacterial population. 2024.04.26.591328 Preprint at https://doi.org/10.1101/2024.04.26.591328 (2024).
41. Levy, S. F., Ziv, N. & Siegal, M. L. Bet hedging in yeast by heterogeneous, age-correlated expression of a stress protectant. *PLoS Biol* **10**, e1001325 (2012).
42. Korem Kohanim, Y. *et al.* A Bacterial Growth Law out of Steady State. *Cell Reports* **23**, 2891–2900 (2018).
43. Ackermann, M. A functional perspective on phenotypic heterogeneity in microorganisms. *Nat Rev Microbiol* **13**, 497–508 (2015).
44. Elowitz, M. B. Stochastic Gene Expression in a Single Cell. *Science* **297**, 1183–1186 (2002).
45. Balaban, N. Q., Merrin, J., Chait, R., Kowalik, L. & Leibler, S. Bacterial Persistence as a Phenotypic Switch. *Science* **305**, 1622–1625 (2004).
46. Lewis, K. Persister cells, dormancy and infectious disease. *Nat Rev Microbiol* **5**, 48–56 (2007).
47. Gasch, A. P. *et al.* Single-cell RNA sequencing reveals intrinsic and extrinsic regulatory heterogeneity in yeast responding to stress. *PLOS Biology* **15**, e2004050 (2017).

48. Munsky, B., Li, G., Fox, Z. R., Shepherd, D. P. & Neuert, G. Distribution shapes govern the discovery of predictive models for gene regulation. *Proceedings of the National Academy of Sciences* **115**, 7533–7538 (2018).
49. Grimbergen, A. J., Siebring, J., Solopova, A. & Kuipers, O. P. Microbial bet-hedging: the power of being different. *Curr Opin Microbiol* **25**, 67–72 (2015).
50. Kafri, M., Metzl-Raz, E., Jona, G. & Barkai, N. The Cost of Protein Production. *Cell Rep* **14**, 22–31 (2016).
51. Eguchi, Y. *et al.* Estimating the protein burden limit of yeast cells by measuring the expression limits of glycolytic proteins. *eLife* **7**, e34595 (2018).
52. Chao, L., Chen, C. K., Shi, C. & Rang, C. U. Spatial and temporal distribution of ribosomes in single cells reveals aging differences between old and new daughters of Escherichia coli. *eLife* **12**, (2023).
53. Raj, A. & van Oudenaarden, A. Nature, Nurture, or Chance: Stochastic Gene Expression and Its Consequences. *Cell* **135**, 216–226 (2008).
54. Tobisch, S., Glaser, P., Krüger, S. & Hecker, M. Identification and characterization of a new beta-glucoside utilization system in Bacillus subtilis. *J Bacteriol* **179**, 496–506 (1997).
55. Egbert, R., Brettner, L., Zong, D. & Klavins, E. Self-destructive altruism encoded by a synthetic developmental program enables complex feedstock utilization. *For eLife* **(in review)**,.
56. Kunkel, J., Luo, X. & Capaldi, A. P. Integrated TORC1 and PKA signaling control the temporal activation of glucose-induced gene expression in yeast. *Nat Commun* **10**, 3558 (2019).
57. Plank, M. *et al.* Systems level analysis of time and stimuli specific signaling through PKA. *Mol Biol Cell* **35**, ar60 (2024).
58. Kinsler, G. *et al.* Extreme Sensitivity of Fitness to Environmental Conditions: Lessons from #1BigBatch. *J Mol Evol* **91**, 293–310 (2023).
59. Worthan, S. B., McCarthy, R. D. P. & Behringer, M. G. Case Studies in the Assessment of Microbial Fitness: Seemingly Subtle Changes Can Have Major Effects on Phenotypic Outcomes. *J Mol Evol* **91**, 311–324 (2023).
60. Lithgow, G. J., Driscoll, M. & Phillips, P. A long journey to reproducible results. *Nature* **548**, 387–388 (2017).
61. Rosenberg, A. B. *et al.* Single-cell profiling of the developing mouse brain and spinal cord with split-pool barcoding. *Science* eaam8999 (2018) doi:10.1126/science.aam8999.
62. Kaminow, B., Yunusov, D. & Dobin, A. STARsolo: accurate, fast and versatile mapping/quantification of single-cell and single-nucleus RNA-seq data. 2021.05.05.442755 Preprint at https://doi.org/10.1101/2021.05.05.442755 (2021).
63. Hao, Y. *et al.* Integrated analysis of multimodal single-cell data. *Cell* **184**, 3573-3587.e29 (2021).
64. Cherry, J. M. *et al.* Saccharomyces Genome Database: the genomics resource of budding yeast. *Nucleic Acids Res* **40**, D700-705 (2012).
65. Pedreira, T., Elfmann, C. & Stülke, J. The current state of SubtiWiki, the database for the model organism Bacillus subtilis. *Nucleic Acids Research* **50**, D875–D882 (2022).

66. Church, S. H., Mah, J. L., Wagner, G. & Dunn, C. W. Normalizing need not be the norm: count-based math for analyzing single-cell data. *Theory Biosci.* **143**, 45–62 (2024).
67. Getting Started with Seurat. https://satijalab.org/seurat/articles/get_started.html.
68. Zhou, Y. *et al.* Metascape provides a biologist-oriented resource for the analysis of systems-level datasets. *Nat Commun* **10**, 1523 (2019).
69. Created with BioRender.com.
70. Sacerdot, C. *et al.* Impact of ionizing radiation on the life cycle of Saccharomyces cerevisiae Ty1 retrotransposon. *Yeast* **22**, 441–455 (2005).